Animal Nutrition 19 (2024) 25–40

Contents lists available at ScienceDirect

Animal Nutrition

journal homepage: http://www.keaipublishing.com/en/journals/aninu/

Original Research Article

New insights into the mechanisms of iron absorption: Iron dextran uptake in the intestines of weaned pigs through glucose transporter 5 (GLUT5) and divalent metal transporter 1 (DMT1) transporters

Shengting Deng [a, b], Weiguang Yang [a, b], Chengkun Fang [a], Haosheng He [a, b], Jiamin Liu [a, b], Rejun Fang [a, b, *]

[a] College of Animal Science and Technology, Hunan Agricultural University, Changsha 410128, China
[b] Hunan Engineering Research Center of Intelligent Animal Husbandry, Changsha 410128, China

ARTICLE INFO

Article history:
Received 16 January 2024
Received in revised form
17 April 2024
Accepted 3 May 2024
Available online 23 July 2024

Keywords:
Iron dextran
Weaned piglet
Divalent metal transporter 1
Glucose transporter 5
Intestinal iron absorption

ABSTRACT

The purpose of this study was to gain insight into the mechanism of iron dextran (DexFe) absorption in the intestines. A total of 72 piglets (average BW = 7.12 ± 0.75 kg, male to female ratio = 1:1) weaned at 28 d of age were randomly divided into two treatment groups with six replicates for each group. The experimental diets included the basal diet supplemented with 100 mg/kg iron dextran (DexFe group) and the basal diet supplemented with 100 mg/kg $FeSO_4 \cdot H_2O$ (CON group). The experiment lasted for 28 d. The piglets' intestinal iron transport was measured in vitro using an Ussing chamber. Porcine intestinal epithelial cell line (IPEC-J2) cells were used to develop a monolayer cell model that explored the molecular mechanism of DexFe absorption. Results showed that compared to the CON group, the ADG of pigs in the DexFe group was improved ($P = 0.022$), while the F/G was decreased ($P = 0.015$). The serum iron concentration, apparent iron digestibility, and iron deposition in the duodenum, jejunum, and ileum were increased ($P < 0.05$) by dietary DexFe supplementation. Piglets in the DexFe group had higher serum red blood count, hemoglobin, serum iron content, serum ferritin and transferrin levels and lower total iron binding capacity ($P < 0.05$). In the Ussing chamber test, the iron absorption rate of the DexFe group was greater ($P < 0.001$) than the CON group, and there was no significant difference between the DexFe group and the glucose group ($P > 0.05$). Furthermore, when compared to the CON group, DexFe administration improved ($P < 0.05$) *SLC2A5* gene and glucose transporter 5 (GLUT5) protein expression but had no effect ($P > 0.05$) on *SLC11A2* gene or divalent metal transporter 1 (DMT1) protein expression. Once the GLUT5 protein was suppressed, the iron transport rate and apparent permeability coefficient were decreased ($P < 0.05$) in IPEC-J2 monolayer cell models. The findings suggest the effectiveness of DexFe application in weaned piglets and revealed for the first time that DexFe absorption in the intestine is closely related to the glucose transporter GLUT5 protein channel.

1. Introduction

Iron is a trace element that is vital for piglet growth and development (Zhuo et al., 2019). It is involved in the tricarboxylic acid cycle, hemoglobin and myoglobin production, oxygen transport, electron transfer, and many other vital biological processes (Wei et al., 2005; Yu et al., 2019). Piglets require 7 to 16 mg of iron per day for optimal bodily functioning, since their number of red blood cells and other metabolic processes increases during the neonatal and weaning stages (Lipiński et al., 2010). The piglet's body iron reserves are limited, and if no external iron supplement is

* Corresponding author.
E-mail address: zsb@hunau.net (R. Fang).
Peer review under the responsibility of Chinese Association of Animal Science and Veterinary Medicine.

Production and Hosting by Elsevier on behalf of KeAi

https://doi.org/10.1016/j.aninu.2024.05.006

administered, the piglet's chances of developing iron deficiency anemia grow significantly (Perri et al., 2016). The National Research Council (NRC) recommends 100 mg/kg of dietary iron at the moment. Piglets are routinely given iron supplements in two methods throughout development. One strategy is to give neonatal pigs around 200 mg of iron dextran (DexFe) via intravenous injection (Heidbuchel et al., 2019; Wang and Kim, 2012). Another option is to supply pigs with exogenous iron. For many decades, exogenous iron supplements have been employed in livestock breeding. Traditional inorganic ferric salts, such as ferrous sulfate, are chemically unstable and easily mixed with other ingredients in food, resulting in limited biological availability of iron and easy production of free radicals, which causes lipid peroxidation and gastrointestinal adverse effects (Oates and Morgan, 1996). Second-generation iron supplements (iron salts of organic acids), such as ferrous lactate, are absorbed as iron ions and molecular chelates, although they can produce bad responses (Cancelo-Hidalgo et al., 2013), poor stability, and absorption saturation (Liu et al., 2004). Polysaccharide-chelated iron, polypeptide-chelated iron, and amino acid-chelated iron are the primary products of the third generation of iron supplements. The high bioavailability of these iron preparations, such as amino acid-chelated iron, may be related to their chelation composition. This type of iron preparation has superior stability and a higher iron absorption rate than the previous two generations of iron preparations. Researchers suppose this is because chelated iron may be conducted as a whole across a brush-like border membrane, similar to the way small peptides get absorbed by the small intestine (Yu et al., 2019).

Polysaccharide-chelated iron has drawn much attention as a novel kind of iron supplement due to its unique gastrointestinal tolerability and high rate of iron absorption. It has been reported to be beneficial in treating anemia, reducing free radical generation, and modifying the immunological response (Feng et al., 2023; Xian et al., 2018). Furthermore, our previous study revealed that dietary supplementation with polysaccharide iron chelate can enhance the reproductive performance of sows and promote the growth performance of piglets (Deng et al., 2023). Iron dextran has been utilized as a polysaccharide iron supplement since 1954 for intravenous iron supplementation in piglets to prevent anemia (Fletcher and London, 1954), marking nearly seven decades of usage. In 2017, the European Union approved DexFe as a feed additive for pigs (Rychen et al., 2017). One study reported that polysaccharide-iron complexes are absorbed in the form of molecules by the gastrointestinal tract with a high iron absorption rate (Hong et al., 2021). Another recent study explored the in vitro transport pathways of polysaccharide-iron complexes using the Caco-2 cell model and revealed that the *Flammulina velutipes* (polysaccharide-iron (III)) complex is used to treat iron-deficiency anemia after being absorbed via GLUT2 and SGLT1 transporters (Shi et al., 2023). Nevertheless, the specific intestinal absorption and transport mechanisms of oral DexFe have not been elucidated due to limited research in this area.

We hypothesize that the higher bioavailability of DexFe can be attributed to its absorption not only through conventional divalent metal ion channels (DMT1) in the intestine but also through the action of sugar molecules in their entirety, which are associated with proteins involved in intestinal glucose uptake. In this study, we explored the absorption and transport of DexFe in vivo and the Ussing perfusion chamber, and further investigated the mechanism of DexFe absorption utilizing the IPEC-J2 cell monolayer model. Finally, the associated genes were silenced using siRNA transfection to verify the intestinal transport mechanism of DexFe. Our findings provide insight into the potential of developing a novel iron supplement.

2. Materials and methods

2.1. Animal ethics statement

The Animal Care and Use Committee of Hunan Agricultural University (Changsha, China) approved all the experimental methods used in the present study. The protocols were developed in accordance with the National Research Council's Guide for the Care and Use of Laboratory Animals (Bioethics Review Section No. 2023151).

2.2. $FeSO_4{\cdot}H_2O$ and iron dextran samples

$FeSO_4{\cdot}H_2O$, a feed-grade inorganic iron supplement, was obtained from Chengdu Shuxing Feed Co., Ltd. and the iron content of the samples was 29.0%. Iron dextran was produced by the Guangxi Research Institute of Chemical Industry (Guangxi, China) using the technology filed in patent CN 102942638 A, China. In brief, dextran with an average mass of 7000 to 80,000 Da was degraded by dextran enzyme into dextran with an average mass of 3000 to 6000 Da. This dextran was subsequently oxidized and directly complexed with iron compounds, yielding the iron dextran products employed in this investigation, and the iron content of the samples in this test was 38.1%.

2.3. Animals, diets, and experimental design

A total of 72 healthy Duroc × Landrace × Yorkshire weaned piglets (average BW = 7.12 ± 0.75 kg, male:female = 1:1) aged 28 d were randomly divided into two treatment groups with six replicates for each group. The experimental diets included a basal diet supplemented with 100 mg/kg $FeSO_4{\cdot}H_2O$ (CON group) and a basal diet supplemented with 100 mg/kg iron dextran (DexFe group). The supplemental levels were calculated from the iron content. The feed is prepared to meet the nutritional needs of weaned piglets, according to the NRC (2012), and its composition and nutrients are shown in Table 1. The experiment lasted for 28 d. The diets were in the form of pellets (the premix in the basic diet was divided into two halves and then weighed). The dextran iron or ferrous sulfate monohydrate and each equal part of the premix were then mixed in a 100-kg small high-speed mixer based on the amounts of iron given to the two treatments. Finally, the two premixes and remaining treated basal diet are combined evenly and granulated in a large horizontal banded blade mixer. The test animals were housed in the same piglet nursery, with each replicate fed in its feeding cage. Each group had piglets that were equally distributed. The house included independent features for maintaining heat and ventilation, providing drinking water, and cleaning up waste. All the piglets were allowed to consume feed ad libitum and drink freely. Feed was provided at 07:00 and 16:00 every day. Furthermore, insulation lights were employed to keep the house at a temperature of 20 to 25 °C and humidity of 30% to 50%. The nursery was illuminated and evenly distributed.

2.4. Recording and sample collection

On d 1 and 28 after an overnight fast, each piglet was weighed on an empty stomach. We determined the feed conversion ratio by dividing the average daily feed intake (ADFI) by the average daily gain (ADG). Samples of DexFe, basic diet, test diet and fresh feces were collected and stored in a −20 °C freezer until analysis. After weighing all of the piglets on d 28, one pig close to the average weight was chosen from each duplicate to slaughter after being sedated with pentobarbital sodium. Duodenal, jejunal and ileal

Table 1
Basal diet composition and nutritional level of weaned piglets (dry matter basis, %).

Item	Content
Ingredients	
Corn, CP ≥ 8.7%	34.00
Soybean meal, CP ≥ 43.0%	13.00
Flour	14.00
Expanded soybean	7.50
Puffed rice	7.50
Fermented soybean meal	4.00
Soybean oil	2.00
Whey powder	7.00
Glucose	4.00
Salt	0.40
Calcium monophosphate	2.12
L-Lysine (98%)	0.40
L-Lysine (70%)	0.42
DL-Methionine (98%)	0.48
Threonine (98%)	0.28
Tryptophan (98%)	0.04
Choline chloride (50%)	0.10
Complex enzyme[1]	0.76
Premix[2]	2.00
Total	100.00
Calculated composition[3]	
Lysine	1.45
Standard ileal digestible amino acids	1.27
Available P	0.31
Digestible energy, MJ/kg	14.52
Measured composition	
Crude protein	17.31
Calcium	0.57
Total phosphorus	0.54
Iron, mg/kg	47.56

[1] Complex enzyme: xylanase ≥40,000 U/g, protease ≥2000 U/g, β-glucanase ≥2000 U/g, pectinase ≥1500 U/g, β-mannanase ≥500 U/g, amylase ≥100 U/g.
[2] The premix provides per kilogram of diet: vitamin A, 16,000 IU; vitamin D_3, 3000 IU; vitamin E, 90 IU; D-pantothenic acid, 35 mg; vitamin B_2, 10 mg; folic acid, 2.6 mg; niacin, 60 mg; vitamin B_1, 4.4 mg; vitamin B_6, 6.3 mg; biotin, 0.4 mg; vitamin B_{12}, 0.05 mg; copper (copper sulfate), 112.5 mg; zinc (zinc sulfate), 110 mg; manganese (manganese sulfate), 63.5 mg; iodine (calcium iodate), 0.66 mg; selenium (sodium selenite), 0.4 mg.
[3] Data were obtained from the addition of the nutritional content data of various raw materials in the Table of NRC (2012).

samples (2 cm × 2 cm) were collected. The samples were subsequently fixed with 4% paraformaldehyde and stored at room temperature for further analysis.

2.5. Analysis of nutrient composition in feed and feces

The iron content was determined by an atomic absorption spectrophotometer (Vario 6, Thermo Fisher Scientific, Jena, Germany) according to the GB/T 13885-2017 method. The crude protein content was determined according to the China National Standard GB/T 6432-2018. The calcium content was determined according to GB/T 6436-2018. The total phosphorus content was determined according to the GB/T 6437-2018 method.

2.6. Biochemical index detection

The red blood cell (RBC) count, hemoglobin concentration (HGB), mean corpuscular volume (MCV), mean corpuscular hemoglobin (MCH), mean corpuscular hemoglobin concentration (MCHC), coefficient of variation of erythrocyte distribution width (RDW-CV), and standard deviation of red blood cell distribution width (RDW-SD) in the blood were all detected using an auto hematology analyzer (Mindray BC-5000 Vet, Shenzhen Mindray Animal Medical Technology Co., Ltd., Shenzhen, China). Total iron binding capacity (TIBC) was measured with a kit (BC2865, Beijing Solarbio Science and Technology Co., Ltd., Beijing, China); serum iron and non-heme iron were measured with a kit (product numbers: TC1015 100T, non-heme iron product numbers: TC1001 50T, Beijing Leagene Biotechnology Co., Ltd., Beijing, China); serum transferrin and ferritin were measured with a kit (transferrin product numbers: SYP-P0129, ferritin product numbers: SYP-P0113, Xiamen Lunchangshuo Biotechnology Co., Ltd., Xiamen, China).

2.7. Iron content and apparent iron digestibility

The iron content was determined by an atomic absorption spectrophotometer (Vario 6, Thermo Fisher Scientific, Jena, Germany) according to the GB/T 13885-2017 method. In brief, the sample was ashed at 550 ± 15 °C and the residue was dissolved in hydrochloric acid, diluted to a constant volume, and then imported into the air-acetylene flame of the atomic absorption spectrometer. The absorbance of iron was determined, and the content of iron in the solution was calculated according to the concentration of the standard solution. Based on the iron content in the diet and fecal samples, the apparent digestibility of iron was calculated according to the following formula:

$$\text{Apparent digestibility of Iron (\%)} = \left[1 - \left(\frac{\text{dietary acid insoluble ash content}}{\text{acid insoluble ash content in feces}}\right) \times \left(\frac{\text{fecal iron content}}{\text{dietary iron content}}\right)\right] \times 100,$$

where dietary acid insoluble ash content, acid insoluble ash content in feces, fecal iron content, and dietary iron content are all in milligrams per kilogram.

2.8. Prussian blue staining

Following the procedure described by Qiu et al. (2022), 3-mm thick sections of the duodenum, jejunum, and ileum were preserved in 4% paraformaldehyde for paraffin embedding. Following rehydration, the slides were dyed using a Prussian blue dyeing kit (G1424, Chengdu Lilai Biotechnology Co., Ltd., Chengdu, China). The stained slides were digitally photographed using a digital micrograph scanner (Pannoramic 250, 3 DHISTECH, Hungary) after 15 min of incubation in Prussian blue dye solution (G1424, Soleburg, Beijing, China). Nuclear fast red was utilized as an antistaling agent.

2.9. In vitro use of the Ussing chamber permeability test

2.9.1. Instruments and reagents

Instruments including Ussing chamber device (VCC MC6, Beijing Jingong Hongtai Technology Co., Ltd., Beijing, China), a pH meter (SIN-DC2000, Sinomeasure, Hangzhou, China), a digital display constant-temperature water bath (DK-8D, Jiangsu Jinyi Instrument Technology Co., Ltd., Jintan, China), a visible spectrophotometer (L500, Hunan Xiangyi Laboratory Instrument Development Co., Ltd., Changsha, China) were used.

Reagents: 1) For preparation of HEPES-Tris buffer, 6 g of HEPES (R20071, Ameresco, Massachusetts, USA) was weighed and dissolved thoroughly in 800 mL of distilled water. The mixture was then mixed with Tris (CAS: 1185-53-1, Ameresco, Massachusetts, USA) solution (1 mol/L) to adjust the pH to 7.4, and then, 5 mL of 1 mol/L glucose solution was added. The mixture was diluted with distilled water to 1000 mL, mixed, and stored in a refrigerator at 4 °C. 2) For the preparation of 100 mg/L DexFe reserve solution (DexFe group),

ferrous sulfate monohydrate (CON group) and glucose reserve (glucose group) solution: 333.33 mg of ferrous sulfate monohydrate, 262.47 mg of DexFe and 100 mg glucose were weighed, then 1000 mL of distilled water was added until the mixture dissolved. 3) For the preparation of 100 mg/L mannitol reserve solution: 100 mg mannitol was weighed (CAS: 69-65-8, Shanghai Xilong Chemical Co., Ltd., Shanghai, China) and dissolved with an adequate amount of distilled water, before being diluted to a volume of 1000 mL.

2.9.2. Ussing chamber operation procedures

Ussing chamber experiments were performed as described previously (Li et al., 2016). Briefly, at first, a 3% agarose gel (product number: 16500500, Thermo Fisher Scientific, Shanghai, China) was prepared and injected into the electrode head. Second, the electrode was installed, and then the sample clip was inserted, and then HEPES-Tris buffer was added (5 mL on each side), and then the temperature was held constant (37 °C) and the mixture was ventilated (adjusting the flow rate). The Ussing chamber is connected to the voltage and current clamp by the electrode cable. Third, the asymmetric electrode potential and solution resistance were set to zero before the tissue was implanted to enable reliable measurements of physiological parameters once the tissue was installed. Fourth, for collection and installation of the samples, fresh duodenal, jejunal, and ileal samples (within 30 min of dissection) were obtained and cleaned with normal saline and placed in HEPES-Tris buffer solution. The intestinal segment was immediately stripped in HEPES-Tris buffer, and the serous membrane layer on the serous membrane side was removed before the intestinal mucosa was fixed in the diffusion chamber. The computer was connected, and the mixture was allowed to sit for approximately 10 min before 1 mL of the reserved liquid was added to the diffusion pool; 1 mL of mannitol solution at the same concentration was added to the receiving room; and 1 mL of liquid was collected from the diffusion pool and receiving room 30 min later to determine the iron content to be measured. Finally, a digital collection system (Acquire & Analyze 2.3, Acquire, San Francisco, USA) was used to collect intestinal resistance R data in the Ussing chamber circuit system. The iron absorption rate was computed using the following formula:

$$\text{Iron absorption rate (\%)} = [\text{total iron content (mg/L)} - \text{iron retention in diffusion room (mg/L)} - \text{iron content in receiving room (mg/L)}]/\text{total iron content (mg/L)} \times 100.$$

2.10. IPEC-J2 cell culture and establishment of a monolayer model

2.10.1. Instruments and reagents

Inverted phase contrast microscope (Vr3000 Primo Vert, KEYENCE Co., Ltd., Beijing, China), cell resistance meter (Millipore ERS-2, Merck KGaA, Massachusetts, USA), carbon dioxide incubator (HF90, ShangHai Lishen scientific equipment Co. Ltd., Shanghai, China), water bathtub (JHH-2A Leica, Vizla, Germany), ice maker (XD-IMF-40, Xueke Electric Co., Ltd., Changshu, China), fluorescent quantitative PCR instrument (LightCycler480ll, Shanghai Yuanyao Biotechnology Co., Ltd., Basel, Switzerland), electrophoresis instrument (JS94, Beijing Starver Technology Co., Ltd., Beijing, China), high-speed refrigerated centrifuge (Heraeus Fresco 17, Thermo Fisher Scientific, Shanghai, China), and fluorescent enzyme spectrometer (Infinite M PLEX, Shanghai Hao Expansion scientific equipment Co., Ltd., Shanghai, China).

Dulbecco modified eagle medium (DMEM) culture-medium (Meilun Biotechnology Co., Ltd., Shanghai, China), fetal bovine serum (TransGen Biotechnology Co., Ltd., Beijing, China), 100 U/mL penicillin and 100 μg/mL streptomycin dilution (Bioss Biotechnology Co., Ltd., Beijing, China), phosphate buffered saline (Bioss Biotechnology Co., Ltd., Beijing, China), D-Hanks buffer (Biosharp, Labgic Technology Co., Ltd., Beijing, China), CCK8 kit (APExbio Technology LLC, Houston, USA), Transwell culture plate (Corning Biotechnology Co., Ltd., Shanghai, China), EDTA-pancreatic enzyme (Bioss Biotechnology Co., Ltd., Beijing, China), dimethylsulfoxide (DMSO; MP Biomedicals Co., Ltd., California, USA), Trizol (Accurate Biotechnology Co., Ltd., Changsha, China), diethylpyrocarbonate (DEPC) water (Sangon Biotechnology Co., Ltd., Shanghai, China), reverse transcription Kit Evo M-MLV RT Mix Kit AG11728 (Accurate Biology Co., Ltd., Changsha, China), SYBR Green Premix Pro Taq HS qPCR Kit AG11701 (Accurate Biology Co., Ltd., Changsha, China), sodium fluorescein (Meilun Biology Co., Ltd., Dalian, China), alkaline phosphatase (AKP) activity detection kit (Boxbio Science & Technology Co., Ltd., Beijing, China), and transfection kit (riboFECTTMCP, Ribo Biotechnology Co., Ltd., Guangzhou, China).

2.10.2. Experimental design for IPEC-J2 cells

Porcine small intestinal epithelial IPEC-J2 cells (donated by Institute of Subtropical Ecology, Chinese Academy of Sciences, China, Changsha) were cultured as described previously (Liu et al., 2019). In brief, cells were cultured in DMEM (mainly containing 4500 mg/L high glucose, 584 mg/L L-glutamine, 110 mg/L sodium pyruvate, and 15 mg/L phenol red) mixed with 10% fetal bovine serum, 100 U/mL penicillin, and 100 μg/mL streptomycin dilution and were placed in a carbon dioxide incubator at 37 °C, 5% CO_2 concentration and 95% humidity. The culture medium was changed every day, after which cell growth was assessed. The plants were passaged when the growth density was appropriate, and 3- to 8-generation cells in the logarithmic growth phase were selected for the experiment.

2.10.3. Preparation of Fe solutions

The needed amount of DexFe was weighed based on the iron content (38.1%), and ultrapure water was used to dissolve the iron powder, and then the microorganisms were filtered and eliminated using a 0.22-m microporous filter membrane. High-sugar medium containing DMEM (10% fetal bovine serum + 1% double antibody) was then diluted to concentrations of 0.05, 0.1, 0.2, and 0.4 mg/mL. The $FeSO_4H_2O$ solution needed for subsequent testing was prepared in the same manner as DexFe.

2.10.4. Detection of IPEC-J2 cell viability

IPEC-J2 cells were collected at the log growth stage and spread on five 24-well plates, 200 μL of cell suspension per hole, and approximately 5×10^3 cells per hole. After the cells were attached to the wall, the medium was replaced with high-glucose DMEM lacking fetal bovine serum, and the cells were starved for 6 h. Cell viability was determined using the method provided with the CCK8 kit. In brief, when the cell size reached 90%, IPEC-J2 cells were treated for 6, 12, 18, 24, or 30 h with 0, 0.05, 0.1, 0.15, 0.20, or 0.25 mg/mL DexFe solution, after which the original medium containing the treatment reagents was discarded. Then, 100 μL of new media was added to each well, which contained 10 μL of CCK8 reagent, as well as three blank wells of medium devoid of cells. The light absorption at a wavelength of 450 nm was measured using an enzyme label.

2.10.5. Assessment of IPEC-J2 monolayer model

During the course of IPEC-J2 cell culture, the cell growth state and morphology were routinely monitored daily using an inverted phase contrast microscope. IPEC-J2 cells in logarithmic growth were separated into cell suspension and inoculated over a semi-transparent poly (carbon ester) membrane (aperture 0.4 μm,

growing area 0.33 cm^2) in a 12-well Transwell insertion petri dish at a density of 1.0×10^4 cells/cm^2, and 200 μL and 1 mL of complete medium were added to the apical side chamber and the basolateral side chamber, respectively, and the medium was replaced every other day during the first week and once daily after that. Optimal fields of view were selected on the 1st, 7th, 14th, and 21st day of culture in Transwell plates for image capture and documentation. To determine the blank trans epithelial electric resistance (TEER) value, the intrinsic resistance of the polycarbonate ester membrane in the Transwell growth plate was first evaluated using a cell resistance meter, and every three days, the long pole of the electrode from the resistance instrument was positioned vertically outside the Transwell chamber. To determine the TEER, a short pole was set up vertically on the side of the Transwell chamber. The cell TEER value was determined as follows:

TEER value (Ω/cm^2) = [measured TEER value (Ω) − blank TEER value per well (Ω)]/transwell effective membrane area (cm^2).

Alkaline phosphatase activity was detected according to the kit instructions (Boxbio Science & Technology Co., Ltd., Beijing, China). In this test, sodium fluorescein was used as a marker to examine cell permeability. Transwell culture plates with validated TEER values were used in the experiment. Standard curves were created by preparing sodium fluorescein solutions with concentrations of 0, 0.4, 2, 10, and 50 mg/L in D'Hanks buffer and measuring the absorbance at 490 nm using a UV–VIS spectrophotometer. After the Transwell culture plate was washed twice with D'Hanks buffer, 50 mg/L sodium fluorescein produced with D'Hanks buffer (0.2 mL) was added to the apical side, and D'Hanks buffer (1 mL) was added to the basilar side. The samples were cultivated in a carbon dioxide incubator for 30, 60, 90, 120, or 150 min, after which the photometric values and transmittance were computed. The control group was assessed in a blank Transwell culture plate with no cells and the process was the same as that described above.

2.10.6. Iron transport rate and apparent iron permeability coefficient of the cell

Before treating the cells, the iron concentration of the cell mediums was determined to be 0.0073 mg/mL. IPEC-J2 cells that passed the integrity assessment were selected and cultured on Transwell plates. According to the results of the cell viability test, the appropriate concentration of iron solution and appropriate treatment time were selected for IPEC-J2 cells in a carbon dioxide incubator at 37 °C. After that, the culture solutions on the apical side (top membrane) and basilar side (base membrane) side were collected. The iron content was obtained using the method described above, and the iron transport rate and apparent permeability coefficient (Papp) were calculated with the following formulas:

Iron transport rate (%) = (iron content of the basilar side/iron content of the apical side) × 100,

$$Papp = [V/(A \times t)] \times [Fe_{basilar\ side}/Fe_{apical\ side}],$$

where the iron contents of the basilar side and the apical side are in milligrams per milliliter, Papp is in centimeter per second, V is the volume of culture chamber on the base side of Transwell plate (mL), A is the Transwell chambers basilar membrane area (cm^2), t is the handle time for iron solution (s), $Fe_{basilar\ side}$ is the concentration of iron on the base side of Transwell plate (mg/mL), and $Fe_{apical\ side}$ is the concentration of iron on the apical side of Transwell plate (mg/mL).

2.10.7. Cell transfection

The glucose transporter 5 (GLUT5)-targeting double-stranded specific small interfering RNA (siRNA) was produced by RiboBio Co., Ltd., Guangdong, China. The following primer sequences were used: 5′-TGGCAGGCACGATGGAGAAGAT-3′ and 5′-CCTTGGCTGTGG TCTGTCTGTG-3′. Transwell plates were used for IPEC-J2 cell culture. Cells were transfected with riboFECTTM CP reagent (R10035.5, RiboBio Co., Ltd., Guangdong, China) in Opti-MEM supplemented with 100 nmol/L GLUT5 siRNA (Trans group) or negative control siRNA (Non-Trans group) in accordance with the product manuals. And then IPEC-J2 cells of Trans group and Non-Trans group were treated with DexFe solution.

2.11. Quantitative real-time PCR analysis

Total RNA extraction, reverse transcription to cDNA, and real-time quantitative polymerase chain reaction analysis were performed according to the methods of Mazgaj et al. (2021). The primers used were designed with Primer Premier 6.0 software (Table 2). Beta-actin mRNA expression was used to calculate and normalize the values, and the relative mRNA expression was calculated by the $2^{-\Delta\Delta Ct}$ method.

2.12. Western blot analysis

Western blot analysis was performed as previously described (Pu et al., 2022). Briefly, protein was extracted from the duodenum, jejunum, and ileum mucosa using lysis buffer (G2002-100ML, Servicebio Technology Co., Ltd., Wuhan, China). The protein concentration was measured with a BCA protein assay kit (G2026, Servicebio Technology Co., Ltd., Wuhan, China). The protein mixture was added to 5 × reduced protein loading buffer (G2075-100ML, Servicebio Technology Co., Ltd., Wuhan, China) at a ratio of 4:1 and denatured in a boiling water bath for 15 min. Equal amounts of protein were separated via sodium dodecyl sulfate–polyacrylamide gel electrophoresis (SDS–PAGE) and subsequently transferred onto polyvinylidene fluoride membranes. Primary antibodies were incubated overnight at 4 °C, followed by a 2-h incubation with secondary antibodies at room temperature. The band intensities were visualized and determined using a chemiluminescence detection system (6100, CLINX Scientific Instrument Co., Ltd., Shanghai, China). The saved original graph was analyzed by using analysis software (AIWBwell, Servicebio Technology Co., Ltd., Wuhan, China). Primary antibodies used were: β-actin (1:2000, #GB15003, Servicebio technology Co., Ltd., Wuhan, China), divalent metal transporter 1, DMT1 (1:1000, #A10231, ABclonal Technology Co., Ltd., Wuhan, China), hephaestin (Heph) (1:1000, #11148-1-AP, Servicebio technology Co., Ltd., Wuhan, China), GLUT5 (1:1000, #GB114645, Servicebio technology Co., Ltd., Wuhan, China), ferroportin-1, FPN1 (1:1000, #GB111471, Servicebio technology Co., Ltd., Wuhan, China), ATPase Na^+/K^+ transporting subunit alpha 1 (ATP1A1; 1:1000, # BS-9570R, Bioss technology Co., Ltd., Beijing, China), transferrin receptor1 (TfR1; 1:1000, #PB9233, Boster biological engineering Co., Ltd., Wuhan, China). Secondary antibody was anti-rabbit IgG-HRP (GB23303, 1:5000, Servicebio technology Co., Ltd., Wuhan, China). Beta-actin was used as a control for the mean protein concentration.

2.13. Statistical analysis

The data were analyzed using SPSS 26.0 (Chicago, IL, USA). The intestinal resistance and intestinal iron absorption rate were analyzed via one-way ANOVA. Tukey's multiple-range test was used to analyze differences, and when overall differences were significant, Duncan's multiple-range test was used to test the

Table 2
Nucleotide sequences of the primers used to measure the target genes.

Gene symbols	Product length, bp	Accession no.	Nucleotide sequence of primers (5′ to 3′)
SLC11A2	86	XM_021081706.1	F: GGTCCTCATCGTCTGTTCCATCAAC R: CAGCCACCACATACAACACCACAT
SLC40A1	79	XM_003483701.4	F: GCCTGGTTCGGACTGGTCTGAT R: GGCATGAACACGGAGATGACACA
HEPH	139	XM_021079775.1	F: CAGCCATTCAGCATACAGCCTCAT R: GAGCAGGAACTGTCCAGCGATATG
TFRC	195	NM_214001.1	F: GGCTGTATTCTGCTCGTGGA R: AGCCAGAGCCCCAGAAGATA
FTH1	142	NM_001244131.1	F: GCCAAATACTTTCTTCACCA R: CAGTCAGCCCATTCTCCC
CYBRD1	59	XM_005671928.3	F: GCCTTCTGGTTCTGGTGTTTGGG R: CCATTGCGGTCTGGTGACTATCC
SLC2A5	138	XM_021095282.1	F: CCTTGCTGTGGTCTGTGTCTGTG R: TGGCAGGCACGATGGAGAAGAT
ATP1A1	79	XM_021088717.1	F: TCAAGCTGCTACAGAAGAGGAACCT R: AGTTATGATGACGACGGCGGAGA
SLC2A2	82	NM_001097417.1	F: TCTGGTCTCTGTCTGTGTCCATCTT R: CCAAGCCGATCTCCAAGCATCC
SLC5A1	87	XM_021072101.1	F: GCATCTCTACCGCCTGTGTTGG R: GCTTCTTGAATGTCCTCCTCCTCTG
β-Actin	102	XM_021086047.1	F: CCAGCACCATGAAGATCAAGATC R: ACATCTGCTGGAAGGTGGACA

SLC11A2 = solute carrier family 11 member 2; *SLC40A1* = solute carrier family 40 member 1; *HEPH* = hephaestin; *TFRC* = transferrin receptor; *FTH1* = ferritin heavy chain 1; *CYBRD1* = cytochrome b reductase 1; *SLC2A5* = solute carrier family 2 member 5; *ATP1A1* = ATPase Na^+/K^+ transporting subunit alpha 1; *SLC2A2* = solute carrier family 2 member 2; *SLC5A1* = solute carrier family 5 member 1.

differences. Other data were analyzed by Student's *t* test for comparisons between two groups, and the data are shown as the means ± SEM. GraphPad Prism 9 software (v9.5.1; San Diego, CA, USA) was used to construct the bar charts. Statistical significance is denoted by asterisks (*$P < 0.05$, **$P < 0.01$).

3. Results

3.1. Growth performance of weaning piglets

The growth performance of weaned piglets is presented in Table 3. When compared to the CON group, dietary supplementation with DexFe had no effect on the ADFI of the pigs ($P > 0.05$), but improved the final average weight, ADG ($P = 0.022$) and decreased the F/G ($P = 0.015$).

3.2. Iron content and non-heme iron content in tissues and iron apparent digestibility

Compared to the CON group, dietary DexFe supplementation had decreased ($P < 0.05$) the iron content of feces, and increased ($P < 0.05$, Table 4) apparent iron digestibility. Moreover, iron deposition and non-heme iron content in the duodenum, jejunum, ileum, liver, and spleen was significantly increased ($P < 0.05$) by dietary supplements with 100 mg/kg DexFe, with intestinal iron deposition in the duodenum of piglets representing the highest in the two groups.

3.3. Blood indices of weaning piglets

Table 5 reveals the effect of dietary DexFe supplementation on blood iron metabolism indicators in pigs. The serum RBC, HGB, hematocrit (HCT), MCV, MCH, serum iron, ferritin, and transferrin were improved ($P < 0.05$) in the DexFe group compared to the control group. Meanwhile, TIBC was decreased ($P = 0.021$) in DexFe group. However, there were no significant differences in serum MCHC, RDW-CV and RDW-SD between the two groups ($P > 0.05$).

3.4. Results of the Ussing chamber in the intestinal tissue of piglets

Table 6 shows the intestinal tissue resistance and iron absorption of weaned piglets as analyzed by the Ussing chamber. Piglets in the DexFe and glucose groups showed significantly greater ($P < 0.01$) duodenal resistance than piglets in the CON group, but no significant difference in jejunum or ileum resistance were observed ($P > 0.05$). Iron absorption rates in the duodenum, jejunum, and ileum of pigs were significantly greater ($P < 0.05$) in the DexFe and glucose groups compared to the CON group. However, there was no

Table 3
Effects of dietary with iron dextran or ferrous sulfate monohydrate on growth performance of weaned piglets.[1]

Item	Initial average weight, kg	Final average weight, kg	ADFI,[2] g	ADG,[3] g	F/G[4]
DexFe[5]	7.12	18.95[a]	568.65	420.45[a]	1.34[b]
CON[6]	7.13	17.70[b]	544.25	378.24[b]	1.47[a]
SEM	0.122	0.544	26.548	17.975	0.052
P-value	0.919	0.029	0.380	0.022	0.015

[a,b]Means within a column with different superscripts differ ($P < 0.05$).
[1] Data are shown as mean and SEM.
[2] ADFI = average daily feed intake.
[3] ADG = average daily gain.
[4] F/G = average daily feed intake/average daily gain.
[5] DexFe = basal diet + 100 mg/kg Fe in the form of dextran iron.
[6] CON = basal diet + 100 mg/kg Fe in the form of ferrous sulfate monohydrate.

Table 4
Effects of dietary with iron dextran or ferrous sulfate monohydrate on iron content and non-heme iron content in tissues and iron apparent digestibility of weaned piglets.[1]

Item	Iron content, mg/kg							Iron apparent digestibility, %	Non-heme iron content, mg/kg				
	Diet	Feces	Duodenum	Jejunum	Ileum	Liver	Spleen		Duodenum	Jejunum	Ileum	Liver	Spleen
DexFe[2]	148.03	463.37^{b}	56.63^{a}	22.27^{a}	36.34^{a}	136.77^{a}	197.05^{a}	59.89^{a}	33.95^{a}	14.93^{a}	25.82^{a}	46.58^{a}	64.19^{a}
CON[3]	145.51	505.45^{a}	43.81^{b}	18.95^{b}	19.04^{b}	75.57^{b}	169.67^{b}	34.52^{b}	27.74^{b}	9.59^{b}	14.08^{b}	30.82^{b}	45.66^{b}
SEM	6.789	3.986	1.798	0.987	1.947	13.491	5.042	2.212	2.056	2.054	0.675	3.203	2.816
P-value	0.735	<0.001	<0.001	0.037	<0.001	0.001	0.012	<0.001	0.024	0.032	<0.001	0.001	<0.001

^{a,b}Means within column with different superscripts differ ($P < 0.05$).
[1] Data are shown as mean and SEM.
[2] DexFe = basal diet + 100 mg/kg Fe in the form of DexFe.
[3] CON = basal diet + 100 mg/kg Fe in the form of ferrous sulfate monohydrate.

Table 5
Effects of dietary dextran iron (DexFe) supplementation on related indexes of serum iron metabolism in piglets.[1]

Item	RBC, $\times 10^{12}$/L	HGB, g/L	HCT, %	MCV, fL	MCH, pg	MCHC, g/L	RDW-CV, %	RDW-SD, fL	Serum iron, mg/L	Serum ferritin, ng/mL	Serum transferrin, g/L	TIBC, μmol/L
DexFe[2]	5.87^{a}	108.33^{a}	29.43^{a}	50.12^{a}	18.50^{a}	368.83	20.55	39.22	25.15^{a}	117.58^{a}	5.65^{a}	126.98^{b}
CON[3]	5.33^{b}	98.00^{b}	24.90^{b}	47.87^{b}	18.00^{b}	375.45	22.64	39.55	13.85^{b}	37.51^{b}	1.35^{b}	158.81^{a}
SEM	0.194	3.252	0.959	0.630	0.220	2.745	1.075	1.162	0.862	6.168	0.391	9.851
P-value	0.017	0.010	0.001	0.004	0.048	0.056	0.129	0.836	<0.001	<0.001	<0.001	0.021

RBC = red blood cell count; HGB = hemoglobin concentration; HCT = hematocrit; MCV = mean corpuscular volume; MCH = mean corpuscular hemoglobin; MCHC = mean corpuscular hemoglobin concentration; RDW-CV = coefficient of variation of erythrocyte distribution width; RDW-SD = standard deviation of red blood cell distribution width; TIBC = total iron binding capacity.
^{a,b}Means within column with different superscripts differ ($P < 0.05$).
[1] Data are shown as Mean and SEM.
[2] DexFe = basal diet + 100 mg/kg Fe in the form of dextran iron.
[3] CON = basal diet + 100 mg/kg Fe in the form of ferrous sulfate monohydrate.

significant difference in intestinal resistance or iron absorption between the DexFe and glucose groups ($P > 0.05$). Furthermore, through the various intestinal segments, the pigs' intestinal resistance and iron absorption rate were typically in the order of duodenum > jejunum > ileum.

3.5. Intestinal Prussian blue stain

Fig. 1 shows the results of traditional Prussian blue staining of pig's intestinal tissue. Under 10× and 40× microscopes, only the duodenum of piglets in the DexFe group and the CON group exhibited the “blue stain” phenomenon, and the degree of “blue stain” was similar between the two groups. Additionally, no blue stain was observed in the jejunum or ileum segment, indicating the presence of free iron or ferrous ions in the duodenum. However, the jejunum and ileum contained no free iron or ferrous ions.

3.6. Expression of genes and proteins related to glucose/iron absorption and transport in the intestine of piglets

Compared to CON group, the DexFe group's piglets had significantly greater relative expression levels of the solute carrier family 40 member 1 (*SLC40A1*), hephaestin (*HEPH*), and solute carrier family 2 member 5 (*SLC2A5*) genes ($P < 0.05$; Fig. 2A and B) of duodenum, and the ileum had significantly greater relative expression levels of *ATP1A1*, transferrin receptor (*TFRC*) and *HEPH* ($P < 0.01$ Fig. 2C). Furthermore, Western blotting was used to determine the expression of a protein associated with glucose and iron absorption in the pigs' intestines (Fig. 3). Heph, GLUT5, and FPN1 proteins increased in the duodenum and jejunum of DexFe group pigs (Fig. 3A to D), whereas the Heph, TfR1, and ATP1A1 proteins increased in the ileum (Fig. 3E and F) ($P < 0.05$). However, in the duodenum, jejunum, or ileum, there were no significant differences in DMT1 protein expression levels between the two treatment groups ($P > 0.05$).

Table 6
Weaned piglet intestinal tissue resistance and iron absorption assessed by Ussing Chamber.[1]

Item	Intestinal resistance, μΩ			Intestinal iron absorption rate, %		
	Duodenum	Jejunum	Ileum	Duodenum	Jejunum	Ileum
DexFe[2]	371.44^{a}	255.47	150.41	84.21^{a}	80.01^{a}	79.80^{a}
CON[3]	297.28^{b}	244.73	153.38	51.85^{b}	42.45^{b}	38.67^{b}
Glucose[4]	404.53^{a}	271.79	162.08	87.57^{a}	83.22^{a}	79.44^{a}
SEM	17.413	15.735	9.584	4.082	4.677	5.514
P-value	<0.001	0.468	0.692	<0.001	<0.001	<0.001

^{a,b}Means within row with different superscripts differ ($P < 0.05$).
[1] Data are shown as Mean and SEM.
[2] DexFe = 100 mg/L dextran solution treatment group.
[3] CON = 100 mg/L solution of ferrous sulfate monohydrate treatment group.
[4] Glucose = 100 mg/L glucose solution treatment group.

3.7. Determination of the viability of IPEC-J2 cells cultured with different iron concentrations and treatment times

To determine the optimal concentration and duration of DexFe action on IPEC-J2 cells, the prepared DexFe solution was treated at 0 (CON), 0.05 (DexFe0.05), 0.1 (DexFe0.1), 0.2 (DexFe0.2), or 0.4 (DexFe0.4) mg/mL. IPEC-J2 cells were treated for 6, 12, 18, 24, or 30 h, and the results are shown in Fig. 4. The results showed that the cells had optimal viability when they were treated with different doses of DexFe solution for 12 h ($P < 0.05$). Furthermore, compared with those in the CON group, the cell viability in the 0.05 (DexFe0.05), 0.1 (DexFe0.1), 0.2 (DexFe0.2), and 0.4 (DexFe0.4) mg/mL treatment groups improved, and the 0.1 mg/mL DexFe solution treatment group exhibited optimum cell viability.

3.8. Evaluation of the IPEC-J2 cell monolayer

IPEC-J2 cells exhibited a cuboidal or circular shape, a smooth cell surface, no protrusions, and a consistent cell size (Fig. 5A–D). On d 1, enough colonies of digestive passage cells were inoculated on polycarbonate membrane plates in a 24-well Transwell insert Petri dish for culture, and the cell growth density was adequate (Fig. 5A). After 7 d of culture, the cells had merged, and a general pattern of

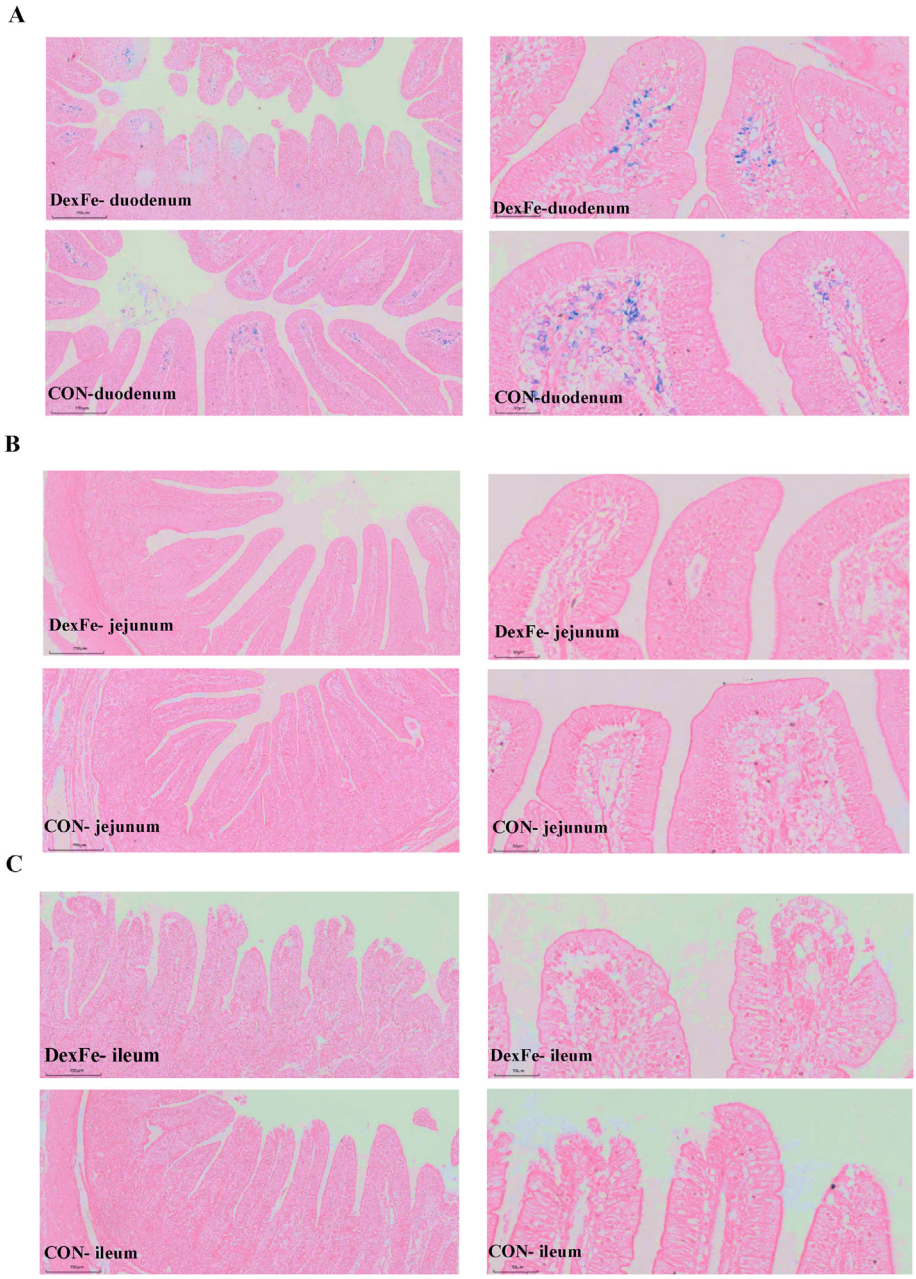

Fig. 1. Distribution of iron in duodenum (A), jejunum (B), ileum (C) of piglets. DexFe, iron dextran group, supplemented with 100 mg/kg iron dextran; CON, control group supplemented with 100 mg/kg ferrous sulfate monohydrate. Sections were observed under magnification 10× (left, scale bar = 200 μm) and 40× (right, scale bar = 50 μm) electron microscopes, respectively. Each group included six replicates.

cross-interconnection was visible (Fig. 5B). The cells were closely packed after 14 d of growth, but there were still gaps, and the cell monolayer was not sufficiently dense (Fig. 5C). After 21 d of incubation, the cells formed a dense cell monolayer (Fig. 5D).

Fig. 5E shows the single-layer TEER values of cells evaluated using a Millipore resistance meter at various culture periods. The TEER value of the cells increased slowly during the first 7 d of growth, and the cells on the Transwell plate did not attach to each other. After 7 to 9 d of incubation, the cells quickly merged, and the TEER increased markedly. The TEER value then gradually increased throughout the 11 to 21 d duration, reaching 413.94 Ω cm^2 at 21 d, showing that the cells had formed a fairly dense monolayer.

On the 11th day of IPEC-J2 proliferation, the AKP activity on the apical side was slightly greater than that on the basilar side (Fig. 5F), indicating that the cells had not yet polarized. On the 21st day of culture, the AKP activity on the apical side was more than three times greater than that on the basilar side. The AKP distribution was quite asymmetric. There was evident polarization and the cells were well differentiated.

The change in the transmittance of sodium fluorescein over time is shown in Fig. 5G. The sodium fluorescein transmission rate in the blank Transwell polycarbonyl ester membrane (cell-free) was very fast. A part of the sodium fluorescein (22.68%) had penetrated in the first 60 min, and the total transmittance was 50.67% after 150 min. The transmittance of sodium fluorescein through 21 d IPEC-J2 cell monolayers was only 0.08% in the first 30 min and the total transmittance was only 1.66% in 150 min.

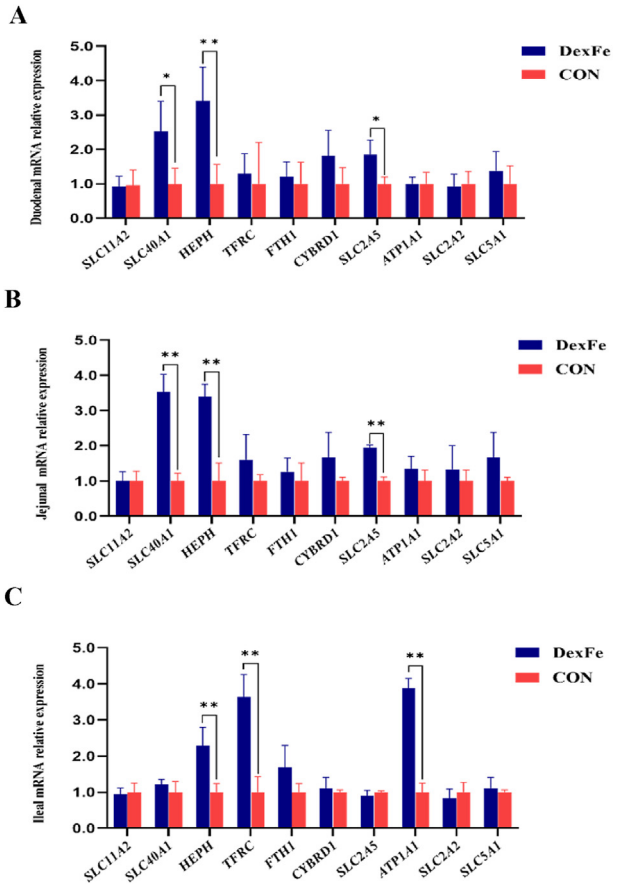

Fig. 2. Relative expression of intestinal gene mRNA. (A) Duodenal mRNA relative expression. (B) Jejunal mRNA relative expression. (C) Ileal mRNA relative expression. DexFe, iron dextran group, supplemented with 100 mg/kg iron dextran. CON, control group supplemented with 100 mg/kg ferrous sulfate monohydrate. *SLC11A2* = solute carrier family 11 member 2; *SLC40A1* = solute carrier family 40 member 1; *HEPH* = hephaestin; *TFRC* = transferrin receptor; *FTH1* = ferritin heavy chain 1; *CYBRD1* = cytochrome b reductase 1; *SLC2A5* = solute carrier family 2 member 5; *ATP1A1* = ATPase Na^+/K^+ transporting subunit alpha 1; *SLC2A2* = solute carrier family 2 member 2; *SLC5A1* = solute carrier family 5 member 1. *Means $P < 0.05$, the difference is significant. **Means $P < 0.01$, the difference is highly significant. Data were presented as mean ± SEM.

3.9. Determination of iron transport in IPEC-J2 cells treated with two iron solutions before transfection test

Before transfection, the Fe transportation rate and Papp of cells in the DexFe group were greater at 37 °C for 12 h when compared to the CON group ($P < 0.05$, Table 7).

3.10. The relative expression of IPEC-J2 cell genes and proteins related to glucose and iron absorption before transfection

Before transfection, the relative expression levels of genes related to iron and glucose absorption are shown in Fig. 6A and B. The relative expression of the glucose absorption-related genes *SLC2A5* and *ATP1A1* in IPEC-J2 cells was increased ($P < 0.01$) after DexFe treatment compared to the control group. However, no effects ($P > 0.05$) were observed on solute carrier family 2 member 2 (*SLC2A2*) or solute carrier family 5 member 1 (*SLC5A1*) expression. While the solute carrier family 11 member 2 (*SLC11A2*), transferrin receptor (*TFRC*), ferritin, *SLC46A1*, and cytochrome b reductase 1 (*CYBRD1*) genes' relative expression levels were not significant ($P > 0.05$), and the *SLC40A1* and *Heph* genes' relative expression levels were significantly higher ($P < 0.01$). Furthermore, we performed Western blotting to measure the relative protein abundance of the cells (Fig. 6C and D) and found that the relative expression levels of Heph, GLUT5, and FPN1 were significantly greater ($P < 0.05$) in the DexFe groups than CON group. However, there was no significant difference in DMT1 protein expression between the two groups ($P > 0.05$).

3.11. The relative expression of differentially expressed genes and proteins in IPEC-J2 cells after transfection

After transfection with siRNA, the relative expression level of the *SLC2A5* gene was decreased ($P < 0.01$), but did not affect the *SLC11A2* gene ($P > 0.05$, Fig. 7A). Similarly, Western blot analysis suggested that transfection decreased GLUT5 protein expression ($P < 0.01$), but DMT1 protein expression was not effect ($P > 0.05$, Fig. 7B and C).

3.12. Determination of iron transport in IPEC-J2 cells treated with two iron solutions after transfection

After transfection, the Fe transportation rate and Papp of IPEC-J2 cells treated with DexFe solutions were analyzed. As assumed, the iron transport rate and Papp in the Trans group were significantly decreased ($P > 0.05$; Table 8), when compared to those in the non-Trans group.

4. Discussion

The ADG was increased during the early postweaning stage, whereas the F/G decreased in response to 100 mg/kg DexFe supplementation in the diet in the current study. These are consistent with our prior findings that polysaccharide iron supplementation can increase piglet growth performance (Deng et al., 2023). This is related to polysaccharide iron complexes being more bioavailable than ferrous sulfate as their structure is more stable and soluble in vitro and in vivo (Cheng et al., 2019; Wang et al., 2015; Zhou et al., 2013).

Two regulatory systems closely control the content of iron in the intestinal mucosa (Tandara and Salamunic, 2012). One of the mechanisms controls intestinal mucosal absorptive cells' (enterocytes') absorption of iron. Iron transport from the basal surface into the blood is then controlled based on the body's current demands. Excess iron entering mucosal cells can be absorbed into ferritin, maintained in intestinal cells for 2 to 3 d, and then eliminated by cell exfoliation and death (Malgorzata et al., 2017). In the present study, the iron levels of the piglet diet were close to the iron availability, while the DexFe supplementation improved the content of iron in the duodenum, jejunum, ileum, liver, and spleen of piglets, indicating that in comparison to ferrous sulfate, DexFe seems to be more readily absorbed by the piglet intestine. Recently, Zeng et al. (2023) found that pigs fed 104 mg/kg yeast iron had substantially greater apparent digestibility than control group receiving a comparable dosage of ferrous sulfate. In piglet studies, Ettle et al. (2008) examined the digestibility of iron glycine, iron chelate, and iron sulfate and found values of 40.9%, 30.8%, and 30.7%, respectively. Similarly, pigs in the DexFe group (58.25%) exhibited higher apparent iron digestibility than those in the CON group (39.89%) in our research. This might be attributed to DexFe's superior solubility and stability in the body.

Generally, the iron absorption and metabolism status of piglets can be assessed by blood indicators, such as RBC, HGB, HCT, MCV, MCH and serum albumin levels (Li et al., 2018). Low RBC and HGB levels are associated with anemia (Bradley et al., 2004; Malgorzata et al., 2017). In the present study, DexFe supplementation increased

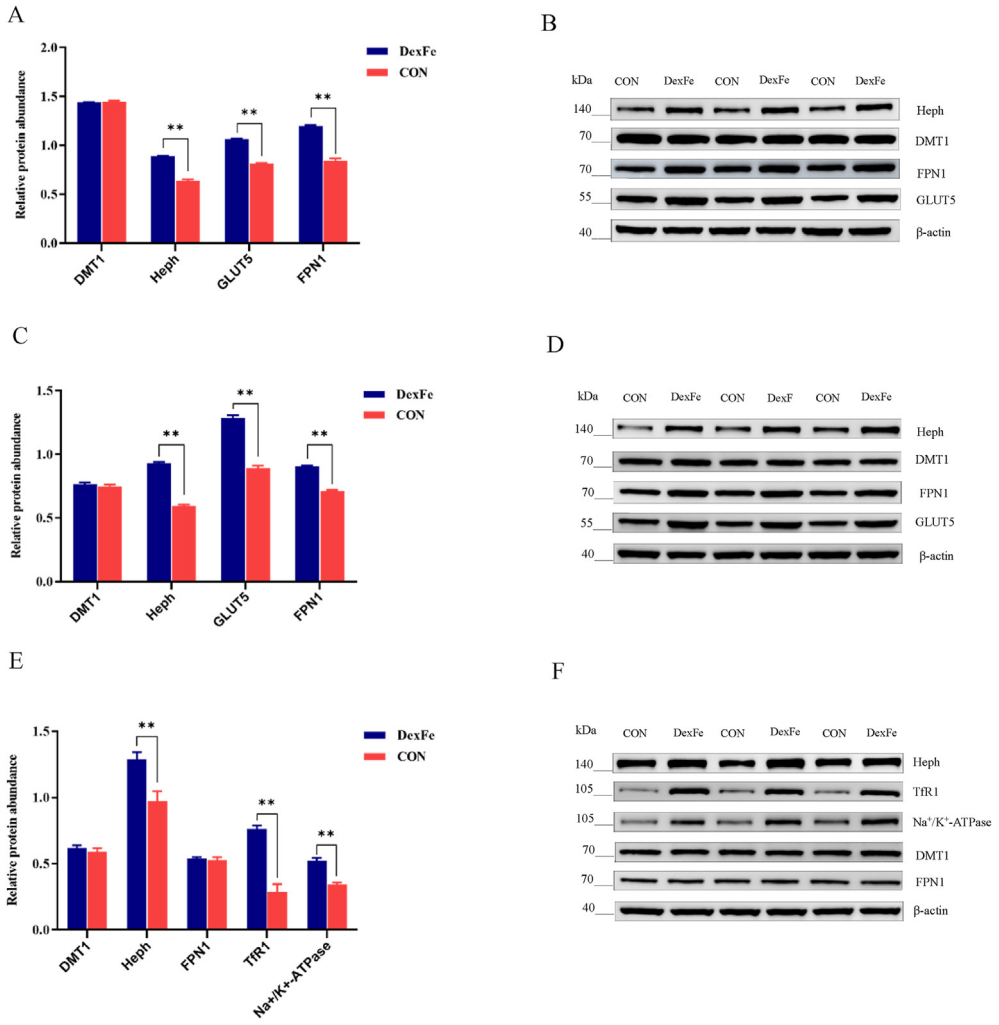

Fig. 3. Western blot analysis of intestinal related protein expression (n = 3). (A–B) Duodenal related protein expression. (C–D) Jejunum-related protein expression levels. (E–F) Expression levels of ileal related proteins. DexFe, iron dextran group, supplemented with 100 mg/kg iron dextran. CON, control group, supplemented with 100 mg/kg ferrous sulfate monohydrate. DMT1 = divalent metal transporter 1; Heph = hephaestin; GLUT5 = glucose transporter 5; FPN1 = ferroportin-1; TfR1 = transferrin receptor1; Na^+/K^+-ATP1A1 = sodium potassium ATPase protein A1; β-actin = beta-actin. Data are presented as the mean ± SEM. *P < 0.05, **P < 0.01.

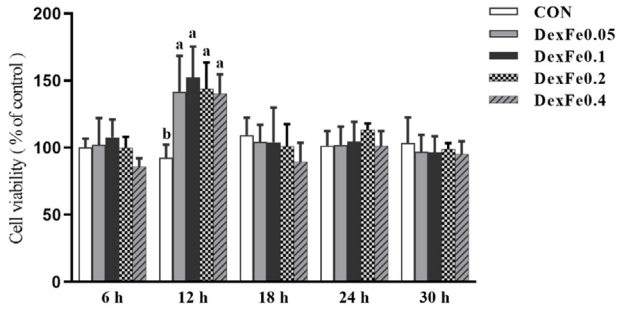

Fig. 4. Results of IPEC-J2 cell viability (n = 12). CON, blank control group, no Fe solution was added. DexFe0.05, DexFe0.1, DexFe0.2, and DexFe0.4 groups were supplemented with 0.05, 0.1, 0.2, and 0.4 mg/kg of dextran-iron solution, respectively. Data are presented as the mean ± SEM. ^{a,b} Different superscripts indicate a significant difference between groups (P < 0.05).

the RBC, HGB, HCT, MCV, MCH, and serum iron contents of piglets, indicating the efficiency of DexFe supplementation in the weaning diet of pigs, these findings are consistent with earlier studies on organic iron (Malgorzata et al., 2017; Sun et al., 2023). The primary form of ferritin stored in piglets is serum ferritin, and its level decreases in anemic animals (Bradley et al., 2004). Transferrin is well known as a key iron-containing protein that regulates iron uptake, storage, and utilization (Smith et al., 1984). The TIBC concentration is the maximum amount of iron that transferrin may bind to 100 mL of serum, and this value increases with anemia (Smith et al., 1984). The amount of iron transported in the serum bound to transferrin is defined by the serum iron concentration, which is reportedly low in patients with iron-deficiency anemia. TR levels are kept high in anemia to improve iron absorption (Luiggi et al., 2014). Previous studies have consistently reported a positive correlation between dietary iron intake and serum ferritin and transferrin levels, accompanied by a concurrent decrease in TIBC values (Li et al., 2018; Luiggi et al., 2014; Sun et al., 2023). In this study, we get the same results as previous studies that piglets in the DexFe group had significantly higher serum ferritin and transferrin levels, whereas TIBC levels were significantly lower. This indicates that DexFe could be efficiently delivered in the blood and utilized by tissues and organs throughout the body.

Few studies have reported dietary iron absorption in the Ussing chamber. Generally, the resistance of the intestine is closely associated with its permeability. Berant et al. (1992) found an increase in overall intestinal permeability among young children during a

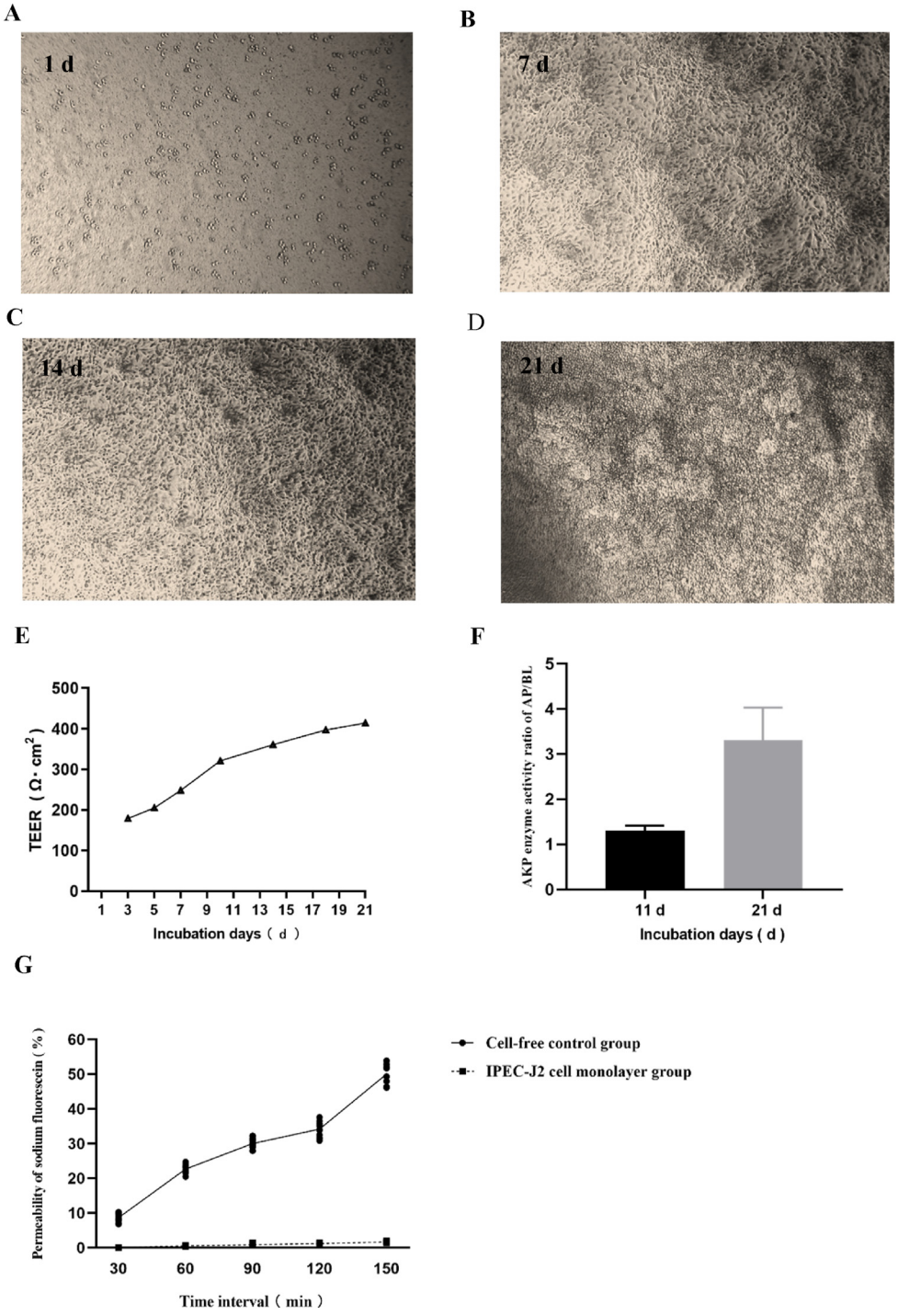

Fig. 5. Results of evaluation index of cell monolayer model. Morphology of IPEC-J2 cells cultured on Transwell plates at 1 d (A), 7 d (B), 14 d (C), and 21 d (D) were observed under optical microscope (40×). (E) Transmembrane resistance (TEER) value curve of IPEC-J2 cells monolayer as a function of time. (F) The alkaline phosphatase (AKP) activity (U/mL) ratio of the IPEC-J2 cell monolayer on d 11 and 21 on the apical side (AP) to basilar side (BL) sides of Transwell plates. (G) The result line graph of fluorescein sodium permeability (AP to BL) change over time in cell-free control group and IPEC-J2 cell monolayer group.

Table 7
Transwell plate after treatment of IPEC-J2 cells with dextran iron (DexFe) and ferrous sulfate monohydrate.[1]

Item	Iron content of cell culture medium, mg/L	Fe transportation rate, %	Fe Papp, $\times 10^{-6}$ cm/s
DexFe[2]	107.74	28.19[a]	4.93[a]
CON[3]	108.39	17.59[b]	2.47[b]
SEM	8.207	1.933	0.706
P-value	0.947	<0.001	0.003

Papp = apparent permeability coefficient.
[a,b]Means within a column with different superscripts differ ($P < 0.05$).
[1] The test was carried out at 37 °C for 12 h, the solution concentrations of DexFe and ferrous sulfate monohydrate were both 0.1 mg/mL, and 12 holes were set up for each treatment (repeat).
[2] DexFe, 0.1 mg/mL DexFe treatment group.
[3] CON, 0.1 mg/mL ferrous sulfate monohydrate treatment group.

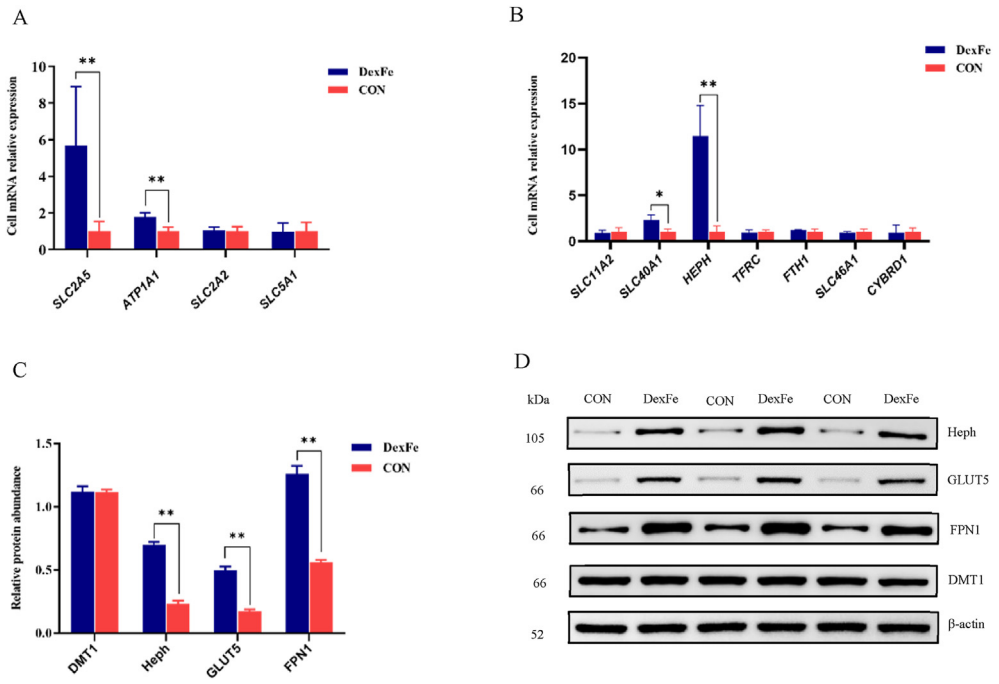

Fig. 6. Histogram of relative expression levels of genes related to glucose (A) and iron (B) absorption before transfection, and the relative expression abundance of related proteins (C) and Western blot analysis (D) before transfection. DexFe, iron dextran group, supplemented with 100 mg/kg iron dextran. CON, control group, supplemented with 0.1 mg/mL ferrous sulfate monohydrate. *SLC2A5* = solute carrier family 2 member 5; *ATP1A1* = ATPase Na^+/K^+ transporting subunit alpha 1; *SLC2A2* = solute carrier family 2 member 2; *SLC5A1* = solute carrier family 5 member 1; *SLC11A2* = solute carrier family 11 member 2; *SLC40A1* = solute carrier family 40 member 1; *HEPH* = hephaestin; *TFRC* = transferrin receptor; *FTH1* = ferritin heavy chain 1; *CYBRD1* = cytochrome b reductase 1; DMT1 = divalent metal transporter 1, Heph = hephaestin, GLUT5 = glucose transporter 5, FPN1 = ferroportin-1. Data are presented as the mean ± SEM. $^{**}P < 0.01$.

state of iron deficiency. A low-iron diet has the potential to attenuate intestinal resistance in piglets (Li et al., 2016). In this study, we found that the resistance of the duodenum was improved in piglets fed DexFe compared with those fed ferrous sulfate monohydrate, demonstrating that the administration of DexFe can improve the development of the duodenal mucosal epithelial barrier in piglets. Furthermore, the intestinal iron absorption rates of the duodenum, jejunum, and ileum increased in the DexFe group, which is consistent with the previously indicated improvement in apparent iron digestibility in pigs in the DexFe group. Interestingly, we noticed that DexFe absorption in the intestines was similar to that of glucose in previous perfusion chamber studies (Herrmann et al., 2012). Thus, we added the glucose group during the Ussing chamber test and confirmed the similarity of DexFe and glucose in intestinal absorption.

Furthermore, we examined the distribution of iron ions in the small intestine using Prussian blue staining. Surprisingly, the ileum, jejunum, and duodenum each exhibited consistent degrees of blue staining, and the ileum and jejunum did not contain any detectable free iron ions. Previous studies suggested that before nonheme iron from the diet can enter intestinal cells through the DMT1 protein, it must first be converted to the form of Fe^{2+} by duodenal cytochrome b (Dcytb) in the intestinal lumen (Frazer and Anderson, 2005). In the present study, the same degree of blue staining indicated that the two groups had similar amounts of ferrous ions in the intestine, whereas the piglets fed DexFe had a greater iron absorption rate, which cannot be explained by the traditional absorption pathway DMT1.

Based on these findings, we hypothesize that intestinal DexFe absorption is closely related to glucose transporter channels and that DexFe may be absorbed into the intestine in the form of polysaccharide molecules as a whole rather than solely dependent on DMT1.

To verify our hypothesis, we focused on probing the relative expression levels of genes involved in iron absorption (*CYBRD*, *SLC11A2*, *HEPH*, *SLC40A1*, *TFRC*, and ferritin heavy chain 1 [*FTH1*]) in

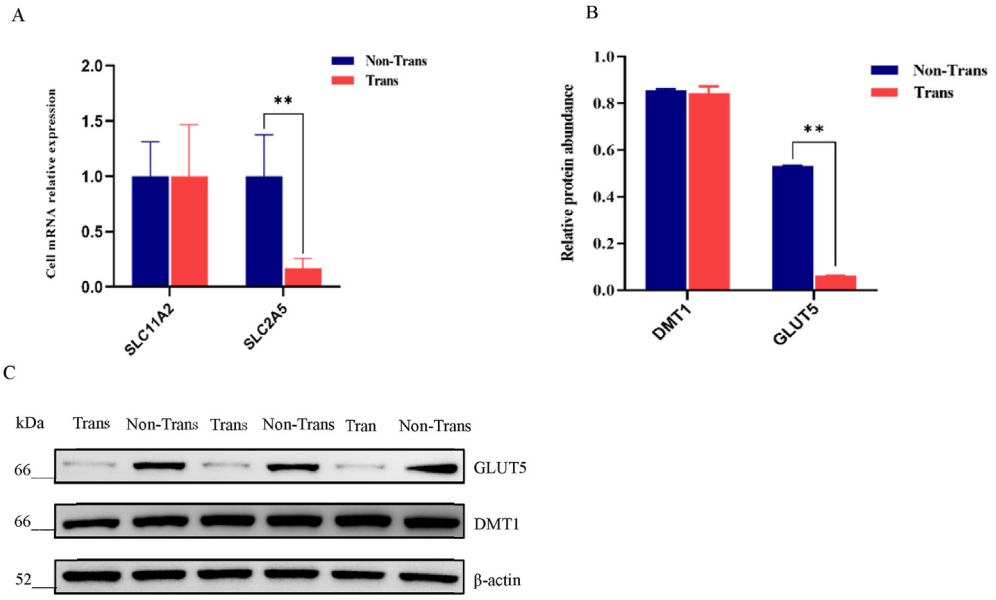

Fig. 7. Histogram of relative expression levels of *SLC11A2* and *SLC2A5* after transfection (A), and the relative expression abundance of DMT1 and GLUT5 proteins (B) and Western blot analysis (C) after transfection. Trans, GLUT5 siRNA transfected test group. Non-Trans, control group transfected without GLUT5 siRNA. *SLC11A2* = solute carrier family 11 member 2; *SLC2A5* = solute carrier family 2 member 5; DMT1 = divalent metal transporter 1; GLUT5 = glucose transporter 5. Data are presented as the mean ± SEM. $^{**}P < 0.01$.

Table 8
Results of iron transport from apical side to basilar side after glucose transporter 5 (GLUT5) siRNA transfection.[1]

Item	Fe transportation rate, %	Fe Papp, $\times 10^{-6}$ cm/s
Trans[2]	11.14[b]	1.56[b]
Non-Trans[3]	23.96[a]	3.36[a]
SEM	0.831	0.117
P-value	<0.001	<0.001

Papp = apparent permeability coefficient.
[a,b]Means within a column with different superscripts differ ($P < 0.05$).
[1] The test was carried out at 37 °C for 12 h, the solution concentrations of DexFe were both 0.1 mg/mL, and 12 holes were set up for each treatment (repeat).
[2] Trans, GLUT5 siRNA transfected test group.
[3] Non-Trans, control group transfected without GLUT5 siRNA.

piglet intestines, as well as genes involved in sugar absorption (*SLC2A5*, *SLC2A2*, *SLC5A1*, and *ATP1A1*). The DMT1 protein and Dcytb enzyme are encoded by the genes *CYBRD* (Luo et al., 2014) and *SLC11A2* (Montalbetti et al., 2013), respectively. The former is a reductase that catalyzes the conversion of iron into ferrous ions, while the latter is a bivalent metal ion transporter across both the plasma and endosomal membranes that serves as the primary channel protein for ferrous ion absorption. *HEPH* and *SLC40A1* encode Heph and Fpn, respectively, where Heph is an iron oxidase protein that converts ferrous iron to iron to promote iron transporter-mediated cellular iron output (Wolkow et al., 2012) and Fpn is the only iron-exporting protein discovered thus far and plays an important role in cellular and systemic iron homeostasis (Ng et al., 2023). *TFRC* (Kaur et al., 2010) and *FTH1* (Palsa et al., 2023) encode transferrin and ferritin, respectively, and are responsible for iron transport and storage in the body. Moreover, the *SLC2A5* (Chalaskiewicz et al., 2023), *SLC2A2* (Sansbury et al., 2012), and *SLC5A1* (Stumpel et al., 1998) encode the GLUT5, GLUT2, and SGLT1 proteins, respectively, which are involved in fructose absorption, glucose transport, and the absorption of glucose and galactose in the intestine, and *ATP1A1* encodes Na^+/K^+-ATPase, an enzyme that generates an ion gradient that contributes to resting membrane potential, maintains cellular excitability, and is vital for intracellular glucose absorption (Moseley et al., 2005). In the present study, the *SLC40A1*, *HEPH*, and *SLC2A5* genes were upregulated in the duodenum and jejunum, as were their encoded proteins FPN1, Heph, and GLUT5, but the expression of DMT1, encoded by *SLC11A2*, was unaffected, suggesting that the duodenum and jejunum are the primary sites of iron absorption. The iron export volume increased significantly in those regions, but it did not contribute to the DMT1 pathway, which may be explained by increased GLUT5 expression. Previous studies have shown that intestinal microbes recycle a small amount of iron in the ileum (Hong et al., 2021). In this study, we noticed significant upregulation of *HEPH*, *TFRC*, and *ATP1A1* gene expression in the ileum, accompanied by an increase in the quantities of Heph, TfR1, and Na^+-K^+ATPase proteins. These findings may help to explain the process of iron utilization by intestinal microbes (Hoppe et al., 2015).

IPEC-J2 is a columnar epithelial cell line derived from the jejunum of newborn pigs. It is a monolayer growing cell line that was initially used in research on epithelial ion transport and cell proliferation (Kandil et al., 1995; Rhoads et al., 1997). IPEC-J2 cells displayed improved permeability, epithelial resistance, and culture properties when cultivated within the polycarbonic acid membrane of a Transwell transport chamber, suggesting that this approach is an appealing choice for an in vitro intestinal absorption and transport model (Marisa et al., 2011). In our study, we exposed IPEC-J2 cells to iron solutions at various concentrations and intervals. Since IPEC-J2 cells showed optimum cell viability after treatment with 0.1 mg/mL Fe solution for 12 h, we followed the procedure for subsequent tests.

Cell morphological characteristics, TEER (Grzeskowiak et al., 2023), AKP activity (Pi et al., 2022), and sodium fluorescein permeability (Bekusova et al., 2021) are commonly employed to examine the integrity of cell monolayers in transport and absorption studies. Previous studies have shown that when the TEER of PEC-J2 cells reaches 400 to 500 Ω cm^2, the cells form a firmly dense monolayer, similar to Caco-2 cells (Vergauwen, 2015). In the present study, IPEC-J2 cells physically resembled intestinal epithelial cells (as detected using an inverted phase contrast microscope), and the transmembrane resistance (413.94 cm^2) and sodium fluorescein permeation rate (1.66%) met the tightness, integrity, and

permeability criteria. Furthermore, AKP activity on the apical side was more than three times that on the basilar side, the AKP distribution was asymmetric, there was obvious polarization, and the cells were differentiated. As a result, the IPEC-J2 model might be used in vitro for further studies.

The Papp value is acknowledged as an indicator for assessing the absorption of drugs in the intestine (Turco et al., 2011). In the IPEC-J2 cell study, we observed that the Fe transport rate and Papp of cells in the DexFe group were greater than those in the CON group, again indicating that DexFe has high bioavailability. Furthermore, after DexFe treatment, the relative expression levels of the *SLC2A5*, *ATP1A1*, *SLC40A1*, and *HEPH* genes increased significantly, as did the expression of Heph, GLUT5, and FPN1. However, the expression levels of the traditional iron transport channel gene *SLC11A2* and the protein DMT1 stayed unaffected, indicating that GLUT5, in addition to the traditional iron channel DMT1, may play an important role in intestinal iron absorption.

To further confirm our hypothesis, we suppressed the expression of the *SLC2A5* gene and the GLUT5 protein but not the traditional iron absorption protein channel DMT1 in the cell transfection test. As expected, compared with the Non-Trans group, the iron transport rate and Papp in the Trans group were significantly decreased. These findings demonstrated that inhibiting GLUT5 could restrict DexFe transport and absorption. Previous studies have reported that both glucose and fructose are potent GLUT5 activators in cells (Douard and Ferraris, 2008; Mesonero et al., 1995), and fructose, lipids, or other nutrients might play a role in regulating gut GLUT5 expression (Song et al., 2023), and iron could be one of those other nutrients. Moreover, polysaccharide-iron complexes are circular, with multicore iron nuclei firmly attached to the internal polysaccharide, producing a core molecule that is surrounded by a mobile external polysaccharide, and polysaccharide-iron complexes usually retain the main structural features of polysaccharides (Shi et al., 2023; Wang et al., 2008). In addition, in the body, polysaccharides hydrolyze into glucose, fructose, and other small molecular. Therefore, the changes in GLUT5 protein levels may be explained by small molecules produced during DexFe metabolism in the gut, such as glucose, fructose, and iron ions. Overall, this finding revealed that not only the DMT1 protein, but also GLUT5, plays an important role in the absorption and transport of DexFe in the intestines.

5. Conclusion

In summary, this study explored the iron transport of DexFe and ferrous sulfate in the intestine of weaned piglets, demonstrated the effectiveness of DexFe application in weaned piglets, and revealed for the first time that DexFe absorption in the intestine is closely related to the glucose transporter GLUT5 protein channel. The study revealed that DexFe may be absorbed into the intestine as a polysaccharide molecule as whole instead of exclusively depending on the bivalent DMT1. However, as this was the first investigation in which DexFe was used in powder form on weaned piglets, relevant research has seen limited reports. The particular upstream and downstream regulatory signaling molecule involved in the GLUT5 protein's DexFe absorption pathway are unknown. Moreover, in this study, only the iron transport in the optimal state of cell vitality was measured in the IPEC-J2 single-layer cell model test, but the influence and rule of different treatment times on cell iron transport were not paid attention to, which is worthy of further exploration in the future. Finally, it is not yet understood what happens when DexFe enters the posterior intestine, or how it would interact with gut microbes, and more research is needed to figure out the complete absorption process of DexFe in intestines.

Author contributions

Shengting Deng conducted the animal experiment and prepared the manuscript draft. **Weiguang Yang, Chengkun Fang, Haosheng He,** and **Jiamin Liu** aided in collecting the samples and laboratory sample testing. **Rejun Fang** contributed to the design of the research and provided financial assistance. All authors have read and approved the final manuscript.

Declaration of competing interest

We declare that we have no financial and personal relationships with other people or organizations that can inappropriately influence our work, and there is no professional or other personal interest of any nature or kind in any product, service and/or company that could be construed as influencing the content of this paper.

Acknowledgments

This study was financially supported by the Hunan Engineering Research Center of Intelligent Animal Husbandry (grant number: 20211231GCZX) of China and Evaluation of the Effectiveness of Iron Dextran Supplementation in Pig Diets (grant number, 2022xczx-214) of Hunan Agricultural University. We thank all members of the Hunan Engineering Research Center of Intelligent Animal Husbandry and Guangxi Research Institute of Chemical Industry Co., Ltd. Nanning, China for their assistance in execution of experiments. We also thank the anonymous reviewers for their constructive comments.

References

Bekusova V, Droessler L, Amasheh S, Markov AG. Effects of 1,2-dimethylhydrazine on barrier properties of rat large intestine and ipec-j2 cells. Int J Mol Sci 2021;22(19):10278. https://doi.org/10.3390/ijms221910278.

Berant M, Khourie M, Menzies IS. Effect of iron deficiency on small intestinal permeability in infants and young children. J Pediatr Gastroenterol Nutr 1992;14(1):17–20. https://doi.org/10.1097/00005176-199201000-00004.

Bradley J, Leibold EA, Harris ZL, Wobken JD, Clarke S, Zumbrennen KB, et al. Influence of gestational age and fetal iron status on irp activity and iron transporter protein expression in third-trimester human placenta. Am J Physiol Regul Integr Comp Physiol 2004;287(4):R894–901. https://doi.org/10.1152/ajpregu.00525.2003.

Cancelo-Hidalgo MJ, Castelo-Branco C, Palacios S, Haya-Palazuelos J, Ciria-Recasens M, Manasanch J, et al. Tolerability of different oral iron supplements: a systematic review. Curr Med Res Opin 2013;29(4):291–303. https://doi.org/10.1185/03007995.2012.761599.

Chalaskiewicz K, Karas K, Zaklos-Szyda M, Karwaciak I, Pastwinska J, Koziolkiewicz M, et al. Trichostatin a inhibits expression of the human *slc2a5* gene *via* snai1/snai2 transcription factors and sensitizes colon cancer cells to platinum compounds. Eur J Pharmacol 2023;949:175728. https://doi.org/10.1016/j.ejphar.2023.175728.

Cheng C, Huang DC, Zhao LY, Cao CJ, Chen GT. Preparation and in vitro absorption studies of a novel polysaccharide-iron (iii) complex from Flammulina velutipes. Int J Biol Macromol 2019;132:801–10. https://doi.org/10.1016/j.ijbiomac.2019.04.015.

China National Standard. Determination of crude protein in feed - Kjeldahl method for nitrogen determination (GB/T 6432-2018). Beijing: Standards Press of China; 2018a.

China National Standard. Determination of calcium in feed (GB/T 6436-2018). Beijing: Standards Press of China; 2018b.

China National Standard. Determination of total phosphorus in feed- Spectrophotometric method (GB/T 6437-2018). Beijing: Standards Press of China; 2018c.

China National Standard. Determination of calcium, copper, iron, magnesium, manganese, potassium, sodium and zinc contents in feed by atomic absorption spectrometry (GB/T 13885-2017). Beijing: Standards Press of China; 2017.

Deng S, Fang C, Zhuo R, Jiang Q, Song Y, Yang K, et al. Maternal supplementary tapioca polysaccharide iron improves the growth performance of piglets by regulating the active components of colostrum and cord blood. Animals (Basel) 2023;13(15):2492. https://doi.org/10.3390/ani13152492.

Douard V, Ferraris RP. Regulation of the fructose transporter glut5 in health and disease. Am J Physiol Endocrinol Metab 2008;295(2):E227–37. https://doi.org/10.1152/ajpendo.90245.2008.

Ettle T, Schlegel P, Roth FX. Investigations on iron bioavailability of different sources and supply levels in piglets. J Anim Physiol Anim Nutr (Berl) 2008;92(1):35–43. https://doi.org/10.1111/j.1439-0396.2007.00707.x.
Feng Y, Wassie T, Wu Y, Wu X. Advances on novel iron saccharide-iron (iii) complexes as nutritional supplements. Crit Rev Food Sci Nutr 2023:1–17. https://doi.org/10.1080/10408398.2023.2222175.
Fletcher F, London E. Intravenous iron. Br Med J 1954;1(4868):984.
Frazer DM, Anderson GJ. Iron imports. I. Intestinal iron absorption and its regulation. Am J Physiol Gastrointest Liver Physiol 2005;289(4):G631–5. https://doi.org/10.1152/ajpgi.00220.2005.
Grzeskowiak L, Vahjen W, Zentek J. Influence of high- and low-fermentable dietary fibres in sows' diet on the colostrum potential against *Clostridioides difficile* toxin-induced effects in ipec-j2 cells. J Anim Physiol Anim Nutr (Berl) 2023;107(6):1376–80. https://doi.org/10.1111/jpn.13834.
Heidbuchel K, Raabe J, Baldinger L, Hagmuller W, Bussemas R. One iron injection is not enough-iron status and growth of suckling piglets on an organic farm. Animals (Basel) 2019;9(9):651. https://doi.org/10.3390/ani9090651.
Herrmann J, Schroder B, Klinger S, Thorenz A, Werner AC, Abel H, et al. Segmental diversity of electrogenic glucose transport characteristics in the small intestines of weaned pigs. Comp Biochem Physiol A Mol Integr Physiol 2012;163(1):161–9. https://doi.org/10.1016/j.cbpa.2012.05.204.
Hong H, Hui T, Qun H, Dan H, Fengping A, Lei C, et al. Beneficial effects of aos-iron supplementation on intestinal structure and microbiota in ida rats. Food Sci Human Wellness 2021;10(1):23–31. https://doi.org/10.1016/j.fshw.2020.05.009.
Hoppe M, Onning G, Berggren A, Hulthen L. Probiotic strain lactobacillus plantarum 299v increases iron absorption from an iron-supplemented fruit drink: a double-isotope cross-over single-blind study in women of reproductive age. Br J Nutr 2015;114(8):1195–202. https://doi.org/10.1017/S000711451500241X.
Kandil HM, Argenzio RA, Chen W, Berschneider HM, Stiles AD, Westwick JK, et al. L-glutamine and l-asparagine stimulate odc activity and proliferation in a porcine jejunal enterocyte line. Am J Physiol 1995;269(4 Pt 1):G591–9. https://doi.org/10.1152/ajpgi.1995.269.4.G591.
Kaur C, Sivakumar V, Ling EA. Expression of tranferrin receptors in the pineal gland of postnatal and adult rats and its alteration in hypoxia and melatonin treatment. Glia 2010;55(3):263–73. https://doi.org/10.1002/glia.20452.
Li Y, Hansen SL, Borst LB, Spears JW, Moeser AJ. Dietary iron deficiency and oversupplementation increase intestinal permeability, ion transport, and inflammation in pigs. J Nutr 2016;146(8):1499–505. https://doi.org/10.3945/jn.116.231621.
Li Y, Yang W, Dong D, Jiang S, Yang Z, Wang Y. Effect of different sources and levels of iron in the diet of sows on iron status in neonatal pigs. Anim Nutr 2018;4(2):197–202. https://doi.org/10.1016/j.aninu.2018.01.002.
Lipiński P, Starzyński RR, Canonne-Hergaux FO, Tudek B, Oliński R, Kowalczyk P, et al. Benefits and risks of iron supplementation in anemic neonatal pigs. Am J Pathol 2010;177(3):1233–43. https://doi.org/10.2353/ajpath.2010.091020.
Liu B, Jiang X, Cai L, Zhao X, Dai Z, Wu G, et al. Putrescine mitigates intestinal atrophy through suppressing inflammatory response in weanling piglets. J Anim Sci Biotechnol 2019;10(69). https://doi.org/10.1186/s40104-019-0379-9.
Liu TC, Lin SF, Chang CS, Yang WC, Chen TP. Comparison of a combination ferrous fumarate product and a polysaccharide iron complex as oral treatments of iron deficiency anemia: a taiwanese study. Int J Hematol 2004;80(5):416–20. https://doi.org/10.1532/ijh97.a10409.
Luiggi FG, Berto DA, Mello GD, Girão LVC, Villela CCEJ, Lo Tierzo V, et al. Relative bioavailability of iron from organic sources for weanling piglets. Semina Ciênc Agrár 2014;35(5):2807. https://doi.org/10.1093/toxsci/kfn084.
Luo X, Hill M, Johnson A, Latunde-Dada GO. Modulation of dcytb (cybrd 1) expression and function by iron, dehydroascorbate and hif-2α in cultured cells. Biochim Biophys Acta Gen Subj 2014;1840(1):106–12. https://doi.org/10.1016/j.bbagen.2013.08.012.
Malgorzata A, Bryszewska MA, Laghi L, Zannoni A, Gianotti A, Barone F, et al. Bioavailability of Microencapsulated Iron from Fortified Bread Assessed Using Piglet Model. Nutrients 2017;9(3):272. https://doi.org/10.3390/nu9030272.
Marisa M, Geenstheo A, Niewold. Optimizing culture conditions of a porcine epithelial cell line ipec-j2 through a histological and physiological characterization. Cytotechnology 2011;63(4):415–23. https://doi.org/10.1007/s10616-011-9362-9.
Mazgaj R, Lipinski P, Szudzik M, Jonczy A, Kopec Z, Stankiewicz AM, et al. Comparative evaluation of sucrosomial iron and iron oxide nanoparticles as oral supplements in iron deficiency anemia in piglets. Int J Mol Sci 2021;22(18):9930. https://doi.org/10.3390/ijms22189930.
Mesonero J, Matosin M, Cambier D, Rodriguez-Yoldi MJ, Brot-Laroche E. Sugar-dependent expression of the fructose transporter glut5 in caco-2 cells. Biochem J 1995;312(3):757–62. https://doi.org/10.1042/bj3120757.
Montalbetti N, Simonin A, Kovacs G, Hediger MA. Mammalian iron transporters: families slc11 and slc40. Mol Aspects Med 2013;34(2–3):270–87. https://doi.org/10.1016/j.mam.2013.01.002.
Moseley AE, Huddleson JP, Bohanan CS, James PF, Lorenz JN, Aronow BJ, et al. Genetic profiling reveals global changes in multiple biological pathways in the hearts of na, k-atpase alpha 1 isoform haploinsufficient mice. Cell Physiol Biochem 2005;15(1–4):145–58. https://doi.org/10.1159/000083647.
Ng S, Lee C, Ng A, Ng S, Arcuri F, House MD, et al. Ferroportin expression and regulation in human placenta/fetal membranes: implications for ferroptosis and adverse pregnancy outcomes. Reprod Biol 2023;23(4):100816. https://doi.org/10.1016/j.repbio.2023.100816.
NRC (National Research Council). Nutrient requirements of swine. 11th ed. Washington, DC: National Academic Press; 2012. p. 232–49.
Oates PS, Morgan EH. Defective iron uptake by the duodenum of belgrade rats fed diets of different iron contents. Am J Physiol 1996;270(5 Pt 1):G826–32. https://doi.org/10.1152/ajpgi.1996.270.5.G826.
Palsa K, Connor JR, Flanagan J, Hines EA. H-ferritin in sows' colostrum- and milk-derived extracellular vesicles: a novel iron delivery concept. J Anim Sci 2023;101:skad013. https://doi.org/10.1093/jas/skad013.
Perri AM, Friendship RM, Harding JCS, O'Sullivan TL. An investigation of iron deficiency and anemia in piglets and the effect of iron status at weaning on post-weaning performance. J Swine Health Prod 2016;24(1):10–20.
Pi G, Song W, Wu Z, Li Y, Yang H. Comparison of expression profiles between undifferentiated and differentiated porcine ipec-j2 cells. Porcine Health Manag 2022;8(1):4. https://doi.org/10.1186/s40813-022-00247-0.
Pu J, Chen D, Tian G, He J, Huang Z, Zheng P, et al. All-trans retinoic acid attenuates transmissible gastroenteritis virus-induced inflammation in ipec-j2 cells via suppressing the rlrs/nf-kappab signaling pathway. Front Immunol 2022;13:734171. https://doi.org/10.3389/fimmu.2022.734171.
Qiu R, Alikhanyan K, Volk N, Marques O, Mertens C, Agarvas AR, et al. Repression of the iron exporter ferroportin may contribute to hepatocyte iron overload in individuals with type 2 diabetes. Mol Metab 2022;66:101644. https://doi.org/10.1016/j.molmet.2022.101644.
Rhoads JM, Argenzio RA, Chen W, Rippe RA, Westwick JK, Cox AD, et al. L-glutamine stimulates intestinal cell proliferation and activates mitogen-activated protein kinases. Am J Physiol 1997;272(5 Pt 1):G943–53. https://doi.org/10.1152/ajpgi.1997.272.5.G943.
Rychen G, Aquilina G, Azimonti G, Bampidis V, Bastos MDL, Bories G, et al. Safety and efficacy of iron dextran as a feed additive for piglets. EFSA J 2017;15(2):e04701. https://doi.org/10.2903/j.efsa.2017.4701.
Sansbury FH, Flanagan SE, Houghton JAL, Shen FLS, Al-Senani AMS, Habeb AM, et al. *slc2a2* mutations can cause neonatal diabetes, suggesting glut2 may have a role in human insulin secretion. Diabetologia 2012;55(9):2381–5. https://doi.org/10.1007/s00125-012-2595-0.
Shi C, Cheng C, Lin X, Qian Y, Du Y, Chen G. *Flammulina velutipes* polysaccharide-iron(iii) complex used to treat iron deficiency anemia after being absorbed via glut2 and sglt1 transporters. Food Sci Human Wellness 2023;12(5):1828–40. https://doi.org/10.1016/j.fshw.2023.02.047.
Smith JE, Moore K, Boyington D, Pollmann DS, Schoneweis D. Serum ferritin and total iron-binding capacity to estimate iron storage in pigs. Vet Pathol 1984;21(6):597–600. https://doi.org/10.1177/030098588402100609.
Song A, Mao Y, Wei H. Glut5: structure, functions, diseases and potential applications. Acta Biochim Biophys Sin (Shanghai) 2023;55(10):1519–38. https://doi.org/10.3724/abbs.2023158.
Stumpel F, Scholtka B, Hunger A, Jungermann K. Enteric glucagon 37 rather than pancreatic glucagon 29 stimulates glucose absorption in rat intestine. Gastroenterology 1998;115(5):1163–71. https://doi.org/10.1016/S0016-5085(98)70087-3.
Sun LM, Yu B, Luo YH, Zheng P, Huang Z, Yu J, et al. Effect of small peptide chelated iron on growth performance, immunity and intestinal health in weaned pigs. Porcine Health Manag 2023;9(1):32. https://doi.org/10.1186/s40813-023-00327-9.
Tandara L, Salamunic I. Iron metabolism: current facts and future directions. Biochem Med 2012;22(3):311–28. https://doi.org/10.11613/bm.2012.034.
Turco L, Catone T, Caloni F, Di Consiglio E, Testai E, Stammati A. Caco-2/tc7 cell line characterization for intestinal absorption: how reliable is this in vitro model for the prediction of the oral dose fraction absorbed in human? Toxicol In Vitro 2011;25(1):13–20. https://doi.org/10.1016/j.tiv.2010.08.009.
Vergauwen H. The ipec-j2 cell line. 2015. p. 125–34. https://doi.org/10.1007/978-3-319-16104-4_12.
Wang J, Chen H, Wang Y, Xing L. Synthesis and characterization of a new inonotus obliquus polysaccharide-iron(iii) complex. Int J Biol Macromol 2015;75:210–7. https://doi.org/10.1016/j.ijbiomac.2015.01.041.
Wang JP, Kim IH. Effects of iron injection at birth on neonatal iron status in young pigs from first-parity sows fed delta-aminolevulinic acid. Anim Feed Sci Technol 2012;178(3–4):151–7. https://doi.org/10.1016/j.aninu.2018.01.002.
Wang K, Chen Z, Zhang Y, Wang P, Wang J, Dai L. Molecular weight and proposed structure of the *Angelica sinensis* polysaccharide-iron complex. Chin J Chem 2008;26(6):1068–74. https://doi.org/10.1002/cjoc.200890189.
Wei KQ, Xu ZR, Luo XG, Zeng LL, Timothy MF. Effects of iron from an amino acid complex on the iron status of neonatal and suckling piglets. Asian Australas J Anim Sci 2005;18(10):1485–91. https://doi.org/10.5713/ajas.2005.1485.
Wolkow N, Song D, Song Y, Chu S, Hadziahmetovic M, Lee JC, et al. Ferroxidase hephaestin's cell-autonomous role in the retinal pigment epithelium. Am J Pathol 2012;180(4):1614–24. https://doi.org/10.1016/j.ajpath.2011.12.041.

Xian H, Wang P, Jing H, Chen GQ, Cheng DF, Ji F, et al. Comparative study of components and anti-oxidative effects between sulfated polysaccharide and its iron complex. Int J Biol Macromol 2018;118(Pt A):1303–9. https://doi.org/10.1016/j.ijbiomac.2018.04.177.

Yu X, Chen L, Ding H, Zhao Y, Feng J. Iron transport from ferrous bisglycinate and ferrous sulfate in dmt1-knockout human intestinal caco-2 cells. Nutrients 2019;11(3):485. https://doi.org/10.3390/nu11030485.

Zeng Y, Jiang L, Zhou B, Liu Y, Wang L, Hu Z, et al. Effect of high efficiency digestion and utilization of organic iron made by saccharomyces cerevisiae on antioxidation and caecum microflora in weaned piglets. Animals (Basel) 2023;13(3):498. https://doi.org/10.3390/ani13030498.

Zhou Y, Liao J, Shen Z. [Absorption, distribution and elimination of (59)Fe-corn polysaccharide iron complex in rats: a study with radioactivity isotope tracing]. Nan Fang Yi Ke Da Xue Xue Bao 2013;33(11):1638–42.

Zhuo Z, Yu X, Li S, Fang S, Feng J. Heme and non-heme iron on growth performances, blood parameters, tissue mineral concentration, and intestinal morphology of weanling pigs. Biol Trace Elem Res 2019;187(2):411–7. https://doi.org/10.1007/s12011-018-1385-z.